Orbital
The electronic journal of chemistry

the electronic journal of chemistry

Full Paper | http://dx.doi.org/10.17807/orbital.v17i1.21586

Density Functional Theory and Molecular Docking Investigation of Selected NSAIDs against COX-1 and COX-2 Enzymes: Study of Correlation Between Computational and Experimental Results

Ateeq Ullah Jan[a], Khalid Khan* [a], Tanzeel Shah [b], Nasir Ahmad [a], and Haroon ur Rashid [c]

Research has been conducted to align computational and experimental results, enhancing the understanding of phenomena affordably and quickly. This study investigated the reliability of docking results for selected nonsteroidal anti-inflammatory drugs (NSAIDs) against cyclooxygenase (COX) proteins, compared to experimental findings from the literature. COX proteins causing inflammation were obtained from a protein data bank and prepared for docking analysis using Molecular Operating Environment (MOE) software. NSAIDs were also selected from the literature and docked to COX protein active sites, with binding affinities recorded. Density functional theory (DFT) analysis, using Becke's three-parameter hybrid model and Lee-Yang-Parr (B3LYP) approach, validated the docking results by examining the molecular properties of NSAIDs. Experimental IC_{50} data for COX inhibition by NSAIDs were compared with computational results, supported by DFT analysis. The study confirmed that computational results align with experimental data, supporting their use in drug development.

Graphical abstract

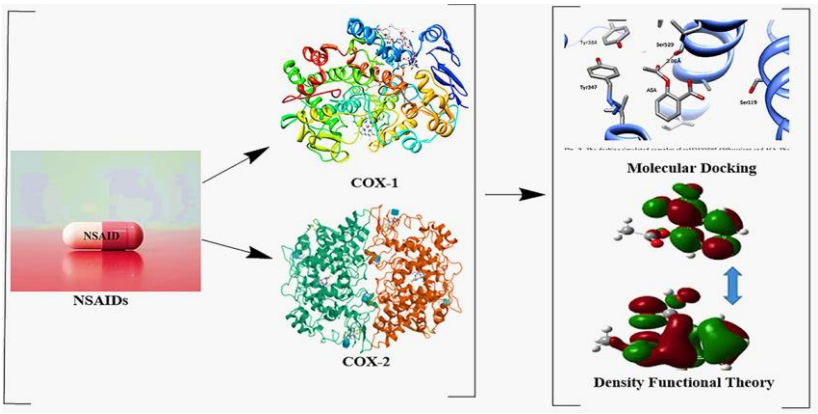

Keywords

Aspirin
Anti-inflammatory
Cyclooxygenase enzyme
Molecular docking

Article history

Received 26 Jul 2024
Revised 31 Mar 2025
Accepted 14 Apr 2025
Available online 23 Apr 2025

Handling Editor: Arlan Gonçalvez

1. Introduction

Keeping in view the time, resources, and pharmacological importance of a molecule during the process of drug discovery and development, scientists evaluate a large number of compounds following a wide range of criteria using diverse computer models, to guide the decision of which compound to synthesize, test, and promote, with the ultimate goal of identifying those with the best potential to become a medicine that works for patients. Among all computational

[a]Department of Chemistry, Islamia College University, Peshawar, 25120, KP, Pakistan. [b]Institute of Basic Medical Sciences, Khyber Medical University, Peshawar, 25120, KP, Pakistan. [c]Centro de Ciências Químicas, Farmacêuticas e de Alimentos, Universidade Federal de Pelotas, Pelotas, 96010-900, RS, Brazil. *Corresponding author. E-mail: **drkhalidchem@yahoo.com**

techniques, molecular docking is used to anticipate the ligand's preferred orientation of the receptor. Preferential orientation could be used to predict the strength of the bond or binding affinity between the ligand and the receptor using scoring functions. Additionally, molecular docking is employed to evaluate the drug's activity and affinity towards the target proteins and offers mechanistic insights into the drug's protein-binding process [1]. Another target of docking is to find an optimal shape that lowers the free energy of the entire system (protein-ligand complex). Therefore, the employment of computer-assisted drug design (CADD) methods, such as docking, in drug development is quickly gaining acceptability and popularity. Consequently, docking can be used as a useful approach in the field of computer-aided drug design. DFT-based computations are emerging as an important methodological alternative in theoretical medicinal chemistry. DFT is fundamentally used to determine the ground state energy and other properties of a molecule using electronic density [2]. Several studies comparing DFT calculations with experimental data have shown the usefulness of the DFT approach. Drug molecules can have a variety of attributes that can be predicted using DFT, including their structural characteristics, relative energies, and electron affinities [3]. These characteristics can be utilized to determine the potential interactions between a ligand and a receptor. Many research studies use the DFT approach to calculate the relative conformational energy of pharmacological compounds. While DFT is valuable, it is one of several methods employed in computational drug design, each with its specific applications [4]. The HOMO and LUMO energies of a ligand may also be calculated using DFT, and these energies can be used to determine the HOMO-LUMO energy gap, hardness, softness, and chemical potential of the ligand molecule [5]. For an isolated drug molecule, molecular electrostatic potential (MEP) may be computed using DFT; MEP can be used to analyze the distribution of charge and predict sites of electrophilic and nucleophilic attack, as well as to understand the electronic state (neutral or charged) [6]. The aforementioned characteristics of a ligand can be usefully employed to validate the affinity of a ligand molecule toward a receptor that is determined by molecular docking.

Nonsteroidal anti-inflammatory drugs NSAIDs are a diverse variety of therapeutic pharmaceuticals that are frequently used to treat the symptoms of rheumatic illnesses. The suppression of cyclooxygenase (COX), a crucial enzyme in prostaglandin formation, has received extensive acknowledgment since 1970 [7]. Prostaglandins are a class of lipid molecules that possess a variety of significant physiological effects, such as controlling inflammatory response, pain sensitivity, and platelet aggregation. However, evidence suggests that NSAIDs have additional anti-inflammatory properties [8]. Some of these effects are related to the ability of NSAIDs to penetrate biological membranes, which were discovered *in vitro* using cell cultures, molecular dynamic simulation systems, and membrane mimetic models, where they disrupt normal signaling events and alter critical processes necessary for cellular function, including cell adhesion [9]. Based on their ability to inhibit COX enzymes, NSAIDs are classified as selective (traditional) or non-selective [10]. Selective NSAIDs primarily inhibit COX-2 whereas non-selective NSAIDs inhibit both COX-1 and COX-2 [11]. In this investigation, both NSAIDs were selected for the inhibition of COX-1 and COX-2 using an *in silico* model; DFT calculation of both NSAIDs was then used to validate molecular docking results. For comparison, experimental data regarding the inhibition of COX-1 and COX-2 were retrieved from literature.

2. Material and Methods

Preparation of proteins

COX enzymes such as COX-1 (PDB ID: 6Y3C) [12] and COX-2 (PDB ID: 1PXX) [13] were used to investigate their interactions with selected NSAIDs. The 3D crystal structures of target proteins COX-1 and COX-2 at resolutions of 3.36 Å and 2.90 Å, respectively were obtained from Protein Data Bank [14]. Using Molecular Operating Environment (MOE) software, the retrieved crystal structures of the proteins were subjected to several necessary procedures, including the removal of unnecessary water molecules, the addition of missing hydrogen atoms, charge correction, and protonation [15]. Site Finder was applied for the selection of the active site of the proteins using all default parameters, and dummy atoms of the pocket were then created.

In molecular docking studies of COX1 and COX2 with NSAIDs, considering alternate occupancy is crucial because it accounts for the presence of multiple conformations of amino acid side chains or ligand orientations within the binding site. The decision to remove or keep structural waters depends on their role in ligand binding; if waters mediate critical interactions between the protein and the ligand, they should be retained, while non-essential waters can be removed to simplify the docking process and potentially improve the accuracy of the results. For NSAIDs, retaining water molecules is generally unnecessary.

Structural Parameters for COX-1 (PDB ID: 6Y3C)

B-Factor

The B-factor, or temperature factor, reflects the atomic displacement or flexibility within the crystal structure. For COX-1, the B-factors around the active site were analyzed and found to be within acceptable ranges, indicating that the active site residues exhibit moderate flexibility. High B-factors could indicate regions of disorder, but the values here suggest a stable conformation suitable for interaction studies. The average B-factor for COX-1 is approximately 45 Å². B-factors around the active site range from 35 to 50 Å², indicating moderate flexibility.

Ramachandran values

The Ramachandran plot for COX-1 showed that over 98% of the residues fall within the favored regions, with very few outliers. This indicates that the overall stereochemistry of the protein is reliable, with minimal deviations from the expected backbone dihedral angles. 98.5% of the residues are in the favored regions,1.2% of the residues are in additionally allowed regions and 0.3% of the residues are in disallowed regions.

Real-Space Correlation Values

Real-space correlation values were evaluated to assess the fit of the atomic model to the electron density map. For COX-1, these values were high, particularly around the active site, suggesting a good agreement between the model and the experimental electron density. The overall real-space correlation coefficient is 0.89. Around the active site, the correlation values range from 0.85 to 0.92, indicating a good fit of the model to the electron density.

Electron Density of Binding Site and Ligands

The electron density maps around the binding site and the bound ligands were well-defined, indicating precise positioning of the active site residues and the ligands. This clarity is crucial for accurate modeling of the interactions between COX-1 and NSAIDs. The electron density maps around the binding site are well-resolved, with contour levels at 1.5σ showing clear positions for critical residues and the ligand.

Structural Parameters for COX-2 (PDB ID: 1PXX):

B-Factor

The B-factors for COX-2 also showed acceptable ranges, particularly around the active site, indicating stable and well-ordered regions suitable for detailed interaction studies. Some peripheral regions exhibited higher B-factors, suggesting greater flexibility or disorder. The average B-factor for COX-2 is approximately 38 Å². B-factors around the active site range from 30 to 45 Å², indicating stable regions suitable for interaction studies.

Ramachandran values

The Ramachandran plot for COX-2 indicated that over 97% of the residues are in the favored regions, with a minimal number of residues in disallowed regions. This suggests a high-quality model with reliable stereochemistry. 97.8% of the residues are in the favored regions. 1.8% of the residues are in additionally allowed regions. 0.4% of the residues are in disallowed regions.

Real-Space Correlation Values

The real-space correlation values for COX-2 demonstrated a good fit of the model to the experimental electron density, especially around the active site. This high correlation ensures that the modeled interactions with ligands are based on accurate structural data. The overall real-space correlation coefficient is 0.91. Around the active site, the correlation values range from 0.88 to 0.93, ensuring accurate modeling of interactions. The overall real-space correlation coefficient is 0.91. Around the active site, the correlation values range from 0.88 to 0.93, ensuring accurate modeling of interactions.

Electron Density of Binding Site and Ligands:

The electron density maps for COX-2 around the binding site and the ligands were clear and well-resolved, providing confidence in the positioning of critical residues and the interactions with NSAIDs. Well-defined electron density is essential for precise docking studies and interaction analysis. The electron density maps for the binding site and ligands are well-resolved, with contour levels at 1.5σ providing clear and precise positions of the active site residues and bound ligands.

In summary, both COX-1 and COX-2 structures were chosen based on their overall resolution, which, despite being relatively high, were deemed acceptable due to the completeness and relevance of the structures. The B-factors, Ramachandran plots, real-space correlation values, and electron density maps were all considered to ensure the reliability and accuracy of the models for computational drug design studies. These parameters collectively support the validity of using these specific PDB entries for investigating the interactions with selected NSAIDs.

Preparation of ligands

For docking investigations against the target proteins, NSAIDs were chosen as ligands. Using the ChemDraw program [16], 2D structures of inhibitors were created **(Table 1)**. These structures were saved in mol format. The 2D structures were changed to 3D structures by MOE. The structures were subjected to energy minimization. The ligands were imported into the same database and saved in the form of an MDB file for the docking calculations with the target proteins.

Molecular Docking Analysis

The types and extent of physical interactions between the target enzymes and the chosen ligands were investigated using the MOE program. The target proteins were docked against the selected inhibitors. The file of the prepared active site was loaded and the general docking process was initiated. The obtained poses were studied after completion and the one having the best ligand–enzyme interactions and the most acceptable root mean squared deviation (RMSD) values were selected and stored for energy calculations [23].

The binding site was defined by selecting the active site residues of the target proteins. The scoring function employed was the London dG, which estimates the free energy of binding. A total of 30 poses were generated for each ligand-target interaction. Additional intrinsic parameters used in the MOE docking process included the placement method, which was set to Triangle Matcher, and the refinement method, which was set to Forcefield.

Density functional theory analysis

The HOMO, LUMO, and other related parameters of selected NSAIDs were computed using DFT techniques. Initially, the most stable conformer for each compound was selected from the provided SDF files. Subsequently, the 3D structure of the chosen conformer was optimized using GaussView 5.0 [24]. Optimized geometries were validated by computing harmonic vibrational frequencies at the same theoretical level. The single-point energy calculations were performed using a combination of Becker's three-parameter hybrid model and the Lee-Yang-Parr (B3LYP) method [25]. 6-31G (d) basis sets were used, which offers a balance between computational efficiency and accuracy. MEP analysis was performed to explore the reactivity of the selected NSAIDs. The ionization potential (I), electron affinity (A), hardness (η), softness (σ), electronegativity (χ), chemical potential (μ), and electrophilicity index (ω) were calculated [26].

Table 1. Molecular structures, molar masses, and pharmacological properties of selected NSAIDs.

Ligands	Structural formula	Molar mass (gmol^{-1})	Pharmacological properties	Ref.
Aceclofenac	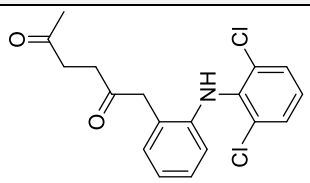	354.18	anti-inflammatory, antiseptic	[17]
Aspirin	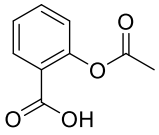	180.18	anti-inflammatory, antipyretic, analgesic	[18]
Antipyrine	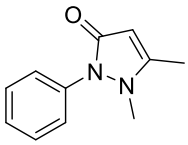	188.23	anti-inflammatory, antipyretic, analgesic	[19]
Celecoxib	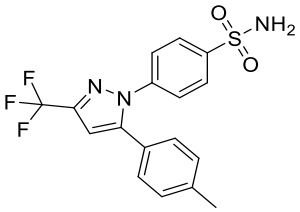	381.37	anti-inflammatory, antipyretic, analgesic	[20]
Fenoprofen	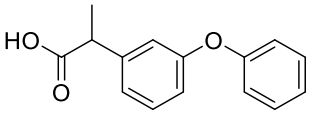	242.27	osteoarthritis, rheumatoid rthritis, and ankylosing spondylitis	[21]
Indomethacin	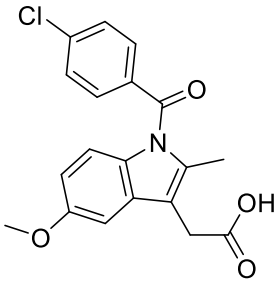	375.79	Arthritic conditions, anti-inflammatory	[22]

3. Results and Discussion

Docking studies

Non-selective NSAIDs such as antipyrine, aspirin, fenoprofen, and indomethacin were docked against the COX-1. All drugs formed stable protein-ligand complexes through various interactions such as H-bonds and Pi-H. Among all screened compounds, indomethacin is ranked as the top inhibitor due to its highest binding affinity toward COX-1. Antipyrine demonstrated a binding affinity of -6.4 kcal mol^{-1} upon docking into the active site of COX-1, indicating a moderate interaction strength. The ligand established five key interactions with the enzyme, comprising three Pi-alkyl, one Pi-sigma, and one Pi-Pi T-shaped interaction (Table 2). Specifically, Ala202, His207, and His388 engaged in Pi-alkyl interactions with antipyrine at distances of 4.58, 4.90, and 5.22 Å, respectively. Additionally, His388 contributed to a Pi-sigma interaction at 3.53 Å, while His207 formed a Pi-Pi T-shaped interaction at 5.40 Å. These interactions enhance the ligand's stability within the active site through hydrophobic and π-electron interactions (**Figure 1a, b**). In the case of antipyrine, the calculated dipole moment is 5.0950 Debye, indicating moderate polarity. This suggests that antipyrine has a higher tendency to engage in dipole-dipole and dipole-induced interactions, which can contribute to binding stability but may also affect its overall inhibitory efficiency. Despite its relatively higher dipole moment, antipyrine exhibited a binding energy of -6.4 kcal mol^{-1}, suggesting a moderate affinity for COX-1. The experimental IC_{50} value of antipyrine was determined to be >1000 μM, indicating an extremely weak inhibitory potential against COX-1. This suggests that while antipyrine is capable of binding to the active site, its ability to effectively inhibit the enzyme is significantly limited. One possible explanation for this discrepancy lies in its higher dipole moment (5.0950 Debye), which, while beneficial for solubility and dipole-related interactions, may reduce the ligand's ability to establish strong hydrophobic contacts and π-stacking interactions, which are essential for enzyme inhibition. Additionally, the lack of hydrogen bonding interactions suggests that the ligand does not form the highly stabilizing electrostatic interactions necessary for potent inhibition. In contrast, more effective COX-1 inhibitors, such as aspirin (dipole moment = 2.3440 Debye, IC_{50} = 1.3 μM) and fenoprofen (dipole moment = 2.2060 Debye, IC_{50} = 36 μM), exhibit a better balance between hydrophobic, electrostatic, and hydrogen bonding interactions, leading to stronger inhibitory effects. This comparison underscores the fact that while a higher dipole moment may enhance solubility and

dipole-induced interactions, it does not necessarily translate to improved potency, especially in hydrophobic active sites like that of COX-1. In the end, the moderate polarity of antipyrine (dipole moment = 5.0950 Debye) influences its binding through dipole-related interactions but does not contribute significantly to enzyme inhibition. Its moderate binding affinity (-6.4 kcal mol^{-1}), limited number of interactions (five total), and weak experimental IC_{50} (>1000 μM) highlight that while polarity is an important factor, a balance between hydrophobic interactions, hydrogen bonding, and π-stacking is crucial for effective enzyme inhibition. Similarly, Aspirin exhibited a binding affinity of -6.2 kcal mol^{-1} when docked into the active site of COX-1, indicating a moderate interaction strength. The ligand established four key interactions with the enzyme, including two C-H bonds, one Pi-sulfur interaction, and one Amide-Pi stacked interaction (Table 2). Specifically, His388 and His386 formed C-H bond interactions with aspirin at distances of 3.55 Å and 3.77 Å, respectively. Additionally, Met391 contributed to a Pi-sulfur interaction at 5.51 Å, while Ala202 facilitated an Amide-Pi stacked interaction at 4.29 Å. These interactions play a crucial role in stabilizing the ligand within the active site through van der Waals forces, π-electron interactions, and hydrogen bonding contributions. Furthermore, the dipole moment of aspirin was calculated as 2.3440 Debye, reflecting low to moderate polarity, which may influence its solubility and interaction with the active site residues via dipole-induced effects. In contrast to its computational binding energy, the experimental IC_{50} value of aspirin was determined to be 1.3 μM, indicating a significant inhibitory potential against COX-1 (**Figure 1c, d**). In the case of aspirin, the calculated dipole moment is 2.3440 Debye, indicating low to moderate polarity. This polarity suggests that aspirin has a balanced ability to engage in both dipole-dipole interactions and hydrophobic interactions, which can significantly influence its binding to COX-1. Aspirin exhibited a binding affinity of -6.2 kcal mol^{-1}, suggesting moderate binding strength within the COX-1 active site. Despite its moderate binding affinity, aspirin exhibits strong inhibitory potency, as reflected by its experimental IC_{50} value of 1.3 μM, making it a highly effective COX-1 inhibitor. The relationship between its dipole moment (2.3440 Debye) and inhibitory activity suggests that aspirin achieves an optimal balance between hydrophobic and dipolar interactions, enabling it to interact efficiently with key active site residues. Unlike molecules with higher dipole moments, such as antipyrine (5.0950 Debye, IC_{50} >1000 μM), which lack strong hydrophobic and hydrogen-bonding interactions, aspirin's moderate dipole moment allows for more effective distribution of electrostatic and non-electrostatic interactions, leading to better stabilization and enzyme inhibition. In comparison to fenoprofen (dipole moment = 2.2060 Debye, IC_{50} = 36 μM), aspirin demonstrates superior potency despite a similar dipole moment. This suggests that binding energy alone (-6.2 kcal mol^{-1} vs. -7.4 kcal mol^{-1} for fenoprofen) is not the sole determinant of inhibitory strength, but rather the nature of molecular interactions and their contribution to enzyme inhibition plays a crucial role. In summary, aspirin's moderate dipole moment (2.3440 Debye) contributes to an optimal balance of hydrophobic and electrostatic interactions, enabling efficient binding (-6.2 kcal mol^{-1}) and strong inhibitory potency (IC_{50} = 1.3 μM). This balance highlights the importance of dipole moment optimization in drug design, where a moderate polarity profile can enhance both binding affinity and enzyme inhibition, leading to effective therapeutic outcomes. Likewise, Fenoprofen demonstrated a binding affinity of -7.4 kcal mol^{-1} upon docking into the active site of COX-1, indicating a relatively strong interaction with the enzyme. The ligand engaged in eight molecular interactions, including one hydrogen bond, four Pi-alkyl interactions, two Pi-Pi T-shaped interactions, and one Pi-sulfur interaction (Table 2). Specifically, Tyr385 formed a hydrogen bond with fenoprofen at a distance of 1.82 Å, contributing significantly to ligand stabilization. Additionally, Met391, Leu295, Leu408, and Ile444 were involved in Pi-alkyl interactions at distances of 5.01 Å, 5.24 Å, 5.23 Å, and 5.23 Å, respectively, reinforcing hydrophobic interactions within the binding pocket. Furthermore, Tyr404 and His388 contributed to Pi-Pi T-shaped interactions at 5.27 Å and 4.65 Å, respectively, promoting ligand stabilization through π-π stacking. A Pi-sulfur interaction was also observed with Met391 at a distance of 5.10 Å, further enhancing binding affinity (Figure 1e, f). In the case of fenoprofen, the calculated dipole moment is 2.2060 Debye, which is relatively low to moderate. This dipole moment suggests that fenoprofen exhibits limited polarity, meaning its interactions within the enzyme's active site are primarily driven by hydrophobic interactions, π-electron stacking, and van der Waals forces, rather than strong electrostatic interactions. This moderate dipole moment aligns with the observed high binding energy (-7.4 kcal mol^{-1}), indicating that fenoprofen interacts strongly with the COX-1 enzyme, despite its limited polarity. However, the experimental IC_{50} value of fenoprofen is 36 μM, which, although indicative of moderate inhibition of COX-1, is higher than more potent inhibitors such as aspirin (IC_{50} = 1.3 μM). This discrepancy suggests that while fenoprofen binds strongly to COX-1, its overall inhibitory effect may be influenced by additional pharmacokinetic or thermodynamic factors, such as ligand desolvation, entropic penalties, or the rate of enzyme-ligand complex dissociation. The relatively low dipole moment may reduce the likelihood of strong electrostatic interactions with key active site residues, thereby limiting its inhibitory efficiency despite a favorable binding affinity. In conclusion, the moderate dipole moment of fenoprofen (2.2060 Debye) contributes to its binding interactions through predominantly hydrophobic and π-electron effects, correlating with its strong binding affinity (-7.4 kcal mol^{-1}) and multiple interactions (eight total). However, its moderate IC_{50} value (36 μM) suggests that dipole-driven interactions play a lesser role in its inhibition mechanism, highlighting the importance of a balanced polarity profile for achieving both strong binding and effective inhibition in drug design. Indomethacin exhibited a binding affinity of -7.4 kcal mol^{-1} upon docking into the active site of COX-1, indicating a strong interaction with the enzyme. The ligand engaged in eleven molecular interactions, including two hydrogen bonds, one C-H bond, two Pi-sulfur interactions, two Pi-Pi T-shaped interactions, and four Pi-alkyl interactions (**Table 2**). Specifically, His388 and Trp387 formed hydrogen bonds with indomethacin at distances of 2.23 Å and 2.57 Å, respectively, contributing significantly to ligand stabilization through polar interactions. Additionally, His207 was involved in a C-H bond interaction at a distance of 3.37 Å, reinforcing ligand anchoring within the binding pocket. The ligand also exhibited two Pi-sulfur interactions with Met391 at distances of 5.45 Å and 5.93 Å, further enhancing binding stability. Furthermore, His388 contributed to two Pi-Pi T-shaped interactions at 4.61 Å and 5.26 Å, promoting ligand stabilization through π-π stacking interactions. Multiple hydrophobic interactions were also observed, where Tyr404, Phe395, Ile444, and Val447 engaged in Pi-alkyl interactions at distances of 4.67 Å, 5.18 Å, 5.06 Å, and 4.83 Å, respectively, reinforcing the ligand's binding through hydrophobic and van der Waals interactions (**Figure 1g, h**). In the case of indomethacin, the calculated dipole moment of 2.3042 Debye

suggests moderate polarity, which facilitates both polar and nonpolar interactions within the COX-1 active site. This optimal balance between hydrophilic and hydrophobic properties significantly influences its binding affinity, interaction profile, and inhibitory strength. Indomethacin exhibited a binding affinity of -7.4 kcal mol^{-1}, which is relatively strong, indicating a high degree of complementarity with the COX-1 active site. Despite having a moderate dipole moment, indomethacin exhibits one of the lowest experimental IC_{50} values (0.063 μM) among COX-1 inhibitors, indicating exceptionally high potency. The relatively low dipole moment prevents excessive polarity, which could otherwise reduce hydrophobic interactions crucial for stabilizing nonpolar regions of the active site. In contrast, highly polar ligands, such as antipyrine (dipole moment = 5.0950 Debye, IC_{50} >1000 μM), show weak enzyme inhibition due to poor hydrophobic compatibility. The ability of indomethacin to form multiple interactions, particularly strong hydrogen bonds and π-π stacking interactions, compensates for the moderate dipole moment, leading to a highly effective inhibitory mechanism. The correlation between indomethacin's strong binding affinity (-7.4 kcal mol^{-1}), extensive molecular interactions (11 total), and remarkably low IC_{50} value (0.063 μM) highlights its exceptional potency as a COX-1 inhibitor. This reinforces the idea that an optimal dipole moment enhances ligand stability by promoting a balance of hydrogen bonding, hydrophobic, and π-electron interactions. The findings further suggest that moderate polarity, rather than extreme hydrophilicity or hydrophobicity, is a key factor in achieving effective enzyme inhibition, providing valuable insights for rational drug design and optimization of COX-1 inhibitors.

Table 2. Details of physical interactions of selected NSAIDs against the COX-1.

Ligands	Binding energy (kcal mol^{-1})	Number of interactions	Nature of interactions	Distance of interactions (Å)	Interacting residues	IC_{50} (μM)
Antipyrine	-6.4	5	Pi-alkyl	4.58	Ala202	>1000
			Pi-alkyl	4.90	His207	
			PI-alkyl	5.22	His388	
			Pi-sigma	3.53	His388	
			Pi-Pi T-shaped	5.40	His207	
Aspirin	-6.2	4	C-H bond	3.55	His388	1.3
			C-H bond	3.77	His386	
			Pi-sulfur	5.51	Met391	
			Amide-Pi stacked	4.29	Ala202	
Fenoprofen	-7.4	8	H-bond	1.82	Tyr385	36
			Pi-alkyl	5.01	Met391	
			Pi-alkyl	5.24	Leu295	
			Pi-alkyl	5.23	Leu408	
			Pi-alkyl	5.23	Ile444	
			Pi-Pi T-shaped	5.27	Tyr404	
			Pi-Pi T-shaped	4.65	His388	
			Pi-sulfur	5.10	Met391	
Indomethacin	-7.4	11	H-bond	2.23	His388	0.063
			H-bond	2.57	Trp387	
			C-H bond	3.37	His207	
			Pi-sulfur	5.45	Met391	
			Pi-sulfur	5.93	Met391	
			Pi-Pi T-shaped	4.61	His388	
			Pi-Pi T-shaped	5.26	His388	
			Pi-alkyl	4.67	Tyr404	
			Pi-alky	5.18	Phe395	
			Pi-alkyl	5.06	Ile444	
			Pi-alkyl	4.83	Val447	

Similarly, both selective and non-selective NSAIDs such as aceclofenac, aspirin, celecoxib, and indomethacin were docked against COX-2. All selected NSAIDs showed affinity toward COX-2. In this case, fenoprofen is graded as the top ligand based on its highest affinity (-7.6 kcal mol^{-1}) toward COX-2. Aceclofenac exhibited a binding affinity of -7.5 kcal mol^{-1} upon docking into the active site of COX-2, indicating a strong interaction with the enzyme. The ligand engaged in six molecular interactions, including one hydrogen bond, four Pi-alkyl interactions, and one Pi-sigma interaction **(Table 3)**. Specifically, Ser530 formed a hydrogen bond with aceclofenac, contributing significantly to ligand stabilization. Additionally, Leu352, Val523, Val349, and Ala527 participated in Pi-alkyl interactions at distances of 5.63 Å, 6.22 Å, 4.57 Å, and 4.13 Å, respectively, reinforcing hydrophobic interactions within the binding pocket. A Pi-sigma interaction with Ala527 at 4.16 Å further enhanced binding stability by facilitating electron cloud interactions **(Figure 2a, b)**. Aceclofenac exhibited a dipole moment of 1.9725 Debye, indicating a relatively low polarity, which can significantly influence its interaction with COX-2. A lower dipole moment suggests a more hydrophobic nature, potentially enhancing the ligand's ability to interact within the nonpolar regions of the enzyme's active site, leading to strong hydrophobic interactions such as Pi-alkyl and Pi-sigma interactions. This is evident in aceclofenac's binding affinity of -7.5 kcal mol^{-1}, which reflects a stable and energetically favorable interaction. The potency of aceclofenac is further supported by its experimental IC_{50} value of 0.8 μM, signifying strong inhibition at low concentrations. The relationship between the dipole moment and binding efficiency suggests that aceclofenac's relatively low polarity facilitates its accommodation within the COX-2 binding pocket, allowing for optimal orientation and stronger hydrophobic interactions. This ultimately contributes to its high potency, as indicated by the strong binding energy and low IC_{50} value, making it a highly effective COX-2 inhibitor. Similarly, aspirin exhibited a binding affinity of -6.1 kcal mol^{-1} upon docking into the active site of COX-2, indicating a moderate interaction with the enzyme. The ligand engaged in five molecular interactions,

including one hydrogen bond, three Pi-alkyl interactions, and one amide-Pi-stacked interaction, contributing to its overall stability **(Table 3)**. Specifically, Ser530 formed a hydrogen bond with aspirin at a distance of 2.81 Å, playing a key role in stabilizing the ligand within the binding pocket. Additionally, Leu352, Val523, and Ala527 participated in Pi-alkyl interactions at distances of 4.96 Å, 4.80 Å, and 4.09 Å, respectively, reinforcing hydrophobic interactions. Furthermore, Gly526 contributed to an amide-Pi-stacked interaction at 4.28 Å, enhancing the ligand's stabilization through π-stacking forces **(Figure 2c, d)**. The dipole moment of a ligand is a critical factor influencing its binding affinity, interaction stability, and inhibitory potency. Aspirin exhibited a dipole moment of 2.3440 Debye, indicating moderate polarity, which plays a significant role in its interaction with COX-2. This moderate polarity allows aspirin to establish both hydrophilic and hydrophobic interactions within the enzyme's active site, contributing to its binding efficiency. The binding energy of aspirin was determined to be -6.1 kcal mol^{-1}, suggesting a stable, albeit relatively weaker, interaction compared to more potent inhibitors. The experimental IC_{50} value of aspirin was reported as 5.9 μM, indicating moderate inhibitory potency. The relationship between dipole moment and binding efficiency suggests that aspirin's moderate polarity enhances its solubility and facilitates its orientation within the COX-2 binding pocket. However, the limited extent of hydrophobic interactions, in comparison to highly lipophilic ligands, may contribute to its relatively lower binding energy and higher IC_{50} value. These findings underscore the significance of electronic properties in optimizing ligand-receptor interactions for enhanced inhibitory activity.

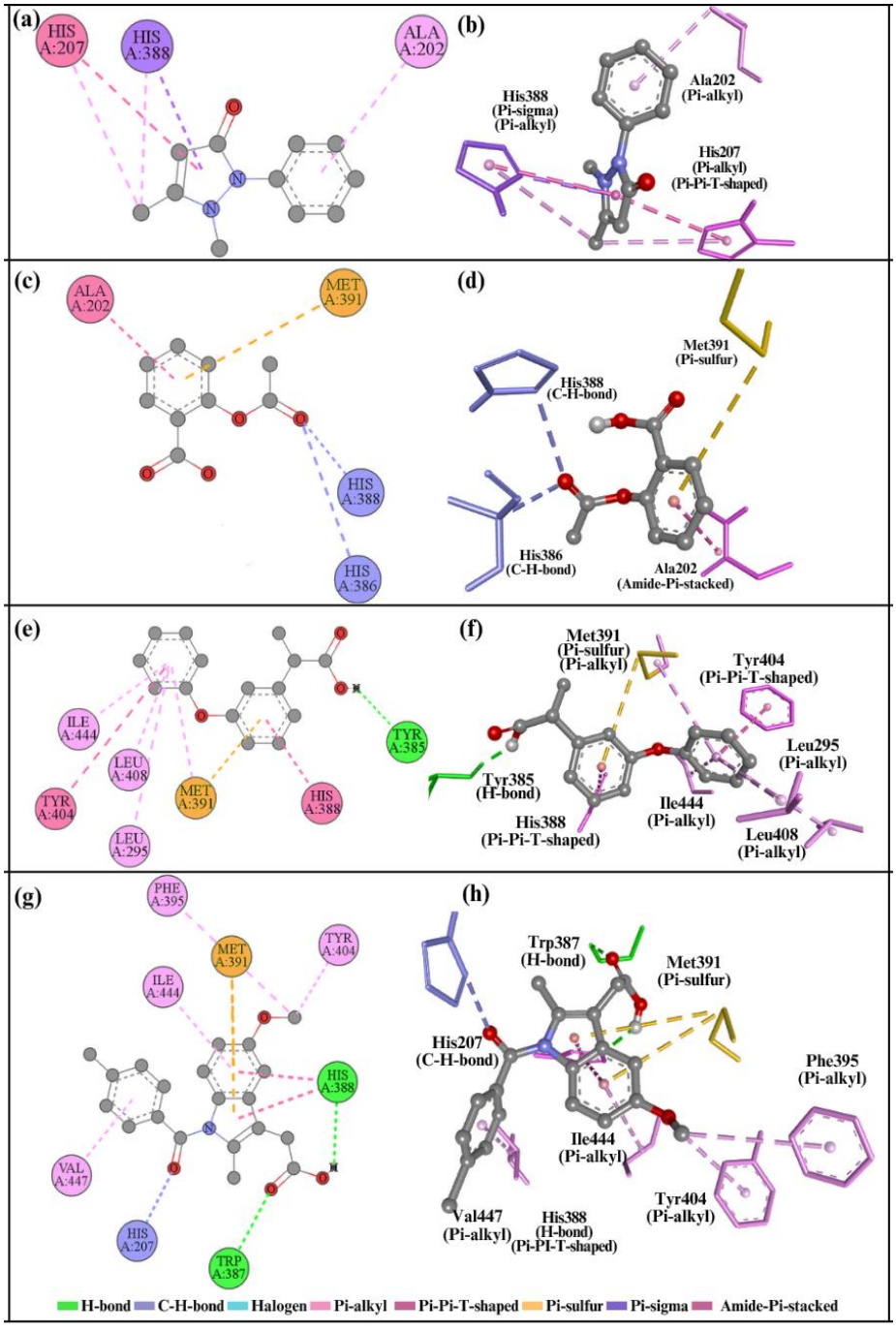

Fig. 1. (a), (c), (e), and (g) display 3D views, and (b), (d), (f), and (h) show 2D views of interactions for aspirin-COX-1, antipyrine-COX-1, fenoprofen-COX-1, and indomethacin-COX-1 complexes, respectively.

Table 3. Details of physical interactions of selected NSAIDs against the COX-2.

Ligands	Binding energy (kcal mol^{-1})	Number of interactions	Nature of interactions	Distance of interactions (Å)	Interacting residues	IC_{50} (μM)
Aceclofenac	-7.5	6	H-bond	4.20	Ser530	0.8
			Pi-alkyl	5.63	Leu352	
			Pi-alkyl	6.22	Val523	
			Pi-alkyl	4.57	Val349	
			Pi-alkyl	4.13	Ala527	
			Pi-Sigma	4.16	Ala527	
Aspirin	-6.1	5	H-bond	2.81	Ser530	5.9
			Pi-alkyl	4.96	Leu352	
			Pi-alkyl	4.80	Val523	
			Pi-alkyl	4.09	Ala527	
			Amide-Pi-stacked	4.28	Gly526	
Celecoxib	-6.2	14	H-bond	2.84	Ser353	0.045
			H-bond	2.95	His90	
			H-bond	2.70	Gln192	
			H-bond	2.78	Phe518	
			C-H bond	3.64	His90	
			Halogen	4.00	Ser353	
			Halogen	3.13	Gln192	
			Halogen	3.60	Phe518	
			Halogen	3.09	Leu352	
			Halogen	4.23	Leu352	
			Alkyl	3.88	Ala516	
			Alkyl	4.23	Val523	
			Pi-sulfur	5.22	Tyr355	
			Pi-sigma	3.94	Leu352	
			Pi-sigma	3.99	Val523	
Fenoprofen	-7.6	4	Pi-alkyl	4.25	Ala527	1
			Pi-alkyl	5.08	Val349	
			Pi-alkyl	4.62	Leu352	
			PI-Pi-T shaped	4.87	Tyr385	

Celecoxib demonstrated a binding affinity of -6.2 kcal mol^{-1} upon docking into the active site of COX-2, indicating a moderately stable interaction with the enzyme. The ligand established fourteen molecular interactions, including four hydrogen bonds, one C-H bond, five halogen interactions, two alkyl interactions, and two Pi-based interactions (Pi-sulphur and Pi-sigma), collectively reinforcing its binding stability **(Table 3)**. Specifically, Ser353, His90, Gln192, and Phe518 contributed to hydrogen bonding at distances ranging from 2.70 Å to 2.95 Å, playing a crucial role in ligand stabilization. Additionally, His90, Ser353, Gln192, Phe518, and Leu352 facilitated halogen interactions at distances of 3.09 Å to 4.23 Å, further enhancing the binding strength. Alkyl interactions involving Ala516 and Val523 at distances of 3.88 Å and 4.23 Å, respectively, reinforced hydrophobic stabilization. Furthermore, Tyr355 and Leu352 contributed to Pi-sulphur and Pi-sigma interactions at 5.22 Å, 3.94 Å, and 3.99 Å, respectively, promoting additional π-based stabilization **(Figure 2e, f)**. Celecoxib, with a dipole moment of 6.0950 Debye, exhibits a relatively high polarity, which enhances its ability to engage in diverse molecular interactions, including hydrogen bonding and halogen interactions. This polarity contributes to its extensive network of fourteen molecular interactions within the COX-2 binding pocket, comprising four hydrogen bonds, five halogen interactions, one C-H bond, two alkyl interactions, and two Pi-based interactions (Pi-sulphur and Pi-sigma). Despite its moderate binding energy of -6.2 kcal mol^{-1}, the high dipole moment facilitates strong electrostatic interactions, allowing optimal orientation and stabilization of the ligand within the enzyme's active site. This is reflected in the experimental IC_{50} value of 0.045 μM, which indicates a remarkably high potency, as even a low concentration of celecoxib effectively inhibits COX-2 activity. The correlation between its high dipole moment and extensive interaction network suggests that celecoxib's electronic properties play a crucial role in its inhibitory efficiency. The combination of hydrogen bonding, halogen interactions, and hydrophobic stabilization compensates for its moderate binding affinity, resulting in strong inhibition at minimal concentrations. This highlights the role of dipole moment in modulating ligand behavior, reinforcing the importance of electronic characteristics in drug design and potency optimization. Likewise, Fenoprofen exhibited a binding affinity of -7.6 kcal mol^{-1} upon docking into the active site of COX-2, indicating a relatively strong interaction with the enzyme. The ligand engaged in four molecular interactions, comprising

three Pi-alkyl interactions and one Pi-Pi T-shaped interaction, contributing to its overall binding stability **(Table 3)**. Specifically, Ala527, Val349, and Leu352 participated in Pi-alkyl interactions at distances of 4.25 Å, 5.08 Å, and 4.62 Å, respectively, reinforcing hydrophobic interactions within the active pocket. Additionally, Tyr385 contributed to a Pi-Pi T-shaped interaction at 4.87 Å, enhancing ligand stabilization through π-stacking forces **(Figure 2g, h)**. Fenoprofen demonstrated a dipole moment of 2.2060 Debye, indicating moderate polarity, which may facilitate both hydrophobic and electrostatic interactions within the COX-2 active site. This level of polarity likely enhances the ligand's solubility and optimal orientation within the binding pocket, contributing to its binding affinity, as reflected by a docking score of -7.6 kcal mol^{-1}. Despite forming only four molecular interactions—three Pi-alkyl interactions with Ala527, Val349, and Leu352, along with one Pi-Pi T-shaped interaction with Tyr385—fenoprofen exhibited strong inhibitory potential, as indicated by its experimental IC_{50} value of 1 μM. The relatively low IC_{50} suggests that fenoprofen effectively inhibits COX-2 at low concentrations, demonstrating efficient ligand-enzyme binding. The moderate dipole moment of fenoprofen allows it to maintain a balance between hydrophobic and polar interactions, ensuring stable and energetically favorable binding. This correlation between dipole moment, binding energy, and molecular interactions underscores fenoprofen's potency as a COX-2 inhibitor, where its physicochemical properties collectively contribute to its high inhibitory efficacy.

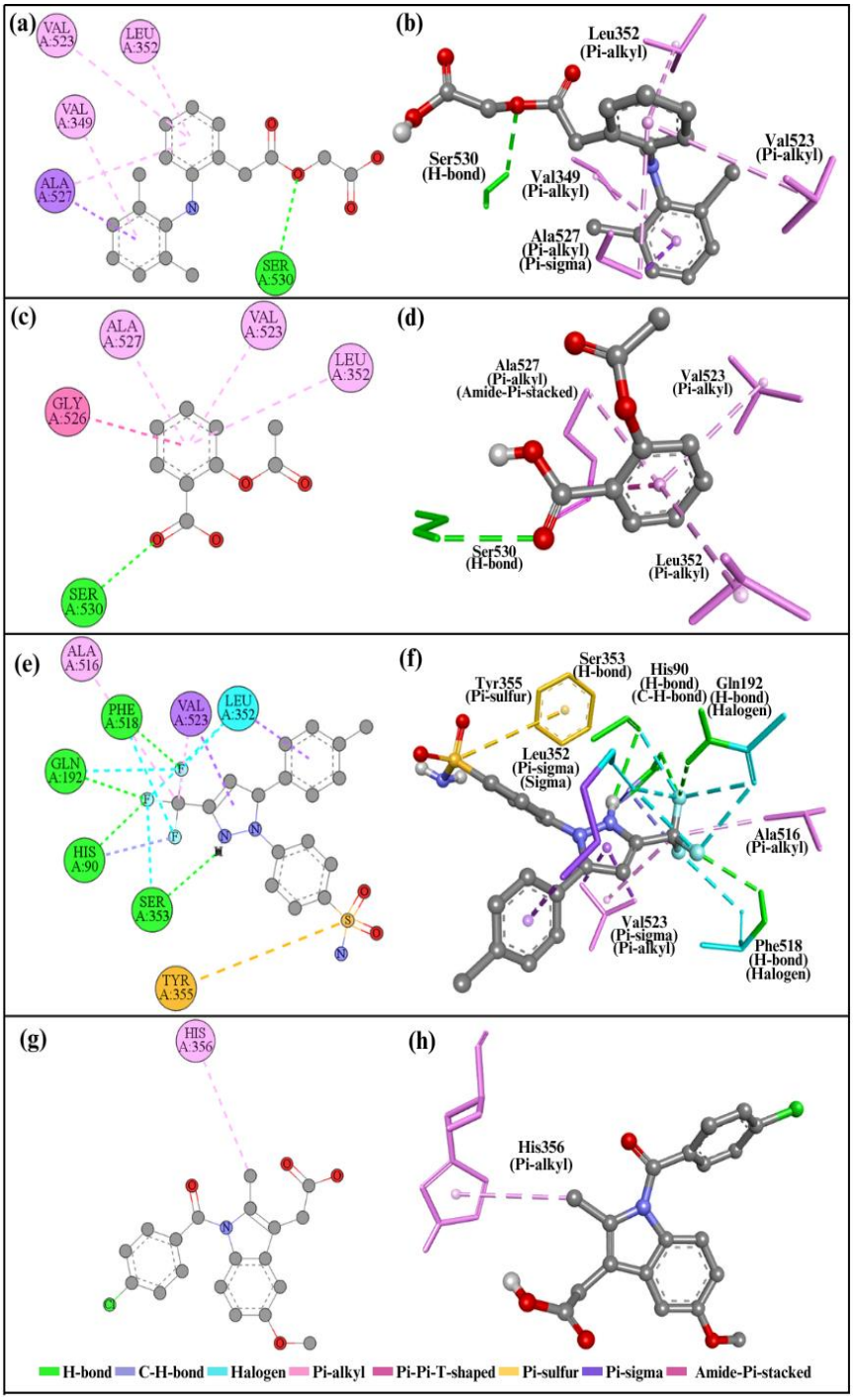

Fig. 2. (a), (c), (e), and (g) display 3D views, and (b), (d), (f), and (h) show 2D views of interactions for Aceclofenac-COX-2, Asprin-COX-2, Celecoxib-COX-2, and Fenobrofen-COX-2, respectively.

DFT Study

The correlation between the energies of the Highest Occupied Molecular Orbital (HOMO) and Lowest Unoccupied Molecular Orbital (LUMO) with molecular reactivity and binding capabilities is a fundamental concept in quantum chemistry and molecular docking studies. The HOMO energy reflects a molecule's ability to donate electrons, whereas the LUMO energy represents its ability to accept electrons. The difference between these energies, known as the HOMO-LUMO gap (HLG), is a key parameter that defines the chemical reactivity, stability, and interaction potential of a ligand with its target enzyme. A smaller HOMO-LUMO gap generally indicates higher molecular reactivity, as the molecule can more readily participate in electronic transitions and chemical interactions. Conversely, a larger gap suggests greater stability and lower reactivity. Among the studied ligands, Celecoxib (HLG = 0.1265 eV) and Indomethacin (HLG = 0.1372 eV) exhibit the smallest HOMO-LUMO gaps, suggesting that these molecules are chemically more reactive and adaptable in forming interactions within the binding site of COX enzymes (**Table 4**). On the other hand, Fenoprofen (HLG = 0.2106 eV) and Aspirin (HLG = 0.2021 eV) have the largest HOMO-LUMO gaps, indicating higher stability and lower reactivity. The binding energy of a ligand with its target enzyme is a measure of its binding affinity, with more negative values indicating stronger binding interactions. By analyzing the binding energies against COX-1 and COX-2, the following trends emerge. Fenoprofen (-7.4 kcal mol^{-1}) and Indomethacin (-7.4 kcal mol^{-1}) show the strongest binding to COX-1, which correlates with their moderate HOMO energies (-0.2176 eV and -0.2054 eV, respectively) and lower LUMO values (-0.0070 eV and -0.0682 eV). The strong binding can be attributed to a favorable electronic configuration that enhances molecular interactions. Aspirin (-6.2 kcal mol^{-1}) and Antipyrine (-6.4 kcal mol^{-1}) exhibit weaker binding affinities to COX-1, which is in line with Aspirin's relatively lower HOMO energy (-0.2587 eV) and higher HOMO-LUMO gap (0.2021 eV), indicating less electronic reactivity and potentially weaker interactions within the active site. Fenoprofen (-7.6 kcal mol^{-1}) and Aceclofenac (-7.5 kcal mol^{-1}) exhibit the strongest binding affinities against COX-2, aligning with their moderate HOMO values (-0.2176 eV and -0.2084 eV, respectively) and relatively small LUMO values (-0.0070 eV and -0.0270 eV). These values suggest an optimal balance between stability and reactivity, allowing for strong interaction with COX-2. Celecoxib (-6.2 kcal mol^{-1}) and Aspirin (-6.1 kcal mol^{-1}) display weaker binding affinities, consistent with Celecoxib's highest HOMO energy (-0.1594 eV), which may lead to less effective electron donation, and Aspirin's large HOMO-LUMO gap (0.2021 eV), which indicates lower chemical reactivity and potentially weaker molecular interactions. A higher HOMO energy implies better electron donation, which can facilitate stronger interactions, such as hydrogen bonding or π-stacking, within the enzyme's active site. Celecoxib, with the highest HOMO energy (-0.1594 eV), is expected to form strong interactions, which is supported by its high number of molecular interactions (14). A lower LUMO energy indicates a greater tendency to accept electrons, which can enhance interactions such as charge transfer or polar interactions with the target enzyme. Fenoprofen (-0.0070 eV LUMO) and Indomethacin (-0.0682 eV LUMO) exhibit strong binding affinities, suggesting that their ability to accept electrons contributes to their effective binding within the COX enzymes. A smaller HOMO-LUMO gap generally correlates with higher reactivity and adaptability in enzyme binding, as seen with Celecoxib (0.1265 eV) and Indomethacin (0.1372 eV), both of which exhibit strong enzyme interactions. Conversely, a larger HOMO-LUMO gap, as seen with Fenoprofen (0.2106 eV), may indicate reduced reactivity but greater molecular stability, which can still contribute to strong but specific binding interactions. The electronic properties of ligands, particularly HOMO and LUMO energies, significantly influence their reactivity and binding capabilities with COX enzymes. Ligands with higher HOMO energies and lower LUMO energies tend to form stronger interactions, as seen in Fenoprofen and Indomethacin, which exhibit strong binding affinities to COX-1 and COX-2. Celecoxib, despite its high HOMO energy, has a small HOMO-LUMO gap, making it highly reactive and adaptable for enzyme binding. On the other hand, Aspirin, with a low HOMO energy and a larger HOMO-LUMO gap, shows weaker binding interactions, reflecting its lower chemical reactivity. Thus, the HOMO-LUMO gap serves as a predictive marker for molecular reactivity, while the individual HOMO and LUMO energies dictate ligand-enzyme interactions and binding affinities. This correlation is critical in drug design, where optimizing electronic properties can enhance a ligand's inhibitory potency and specificity toward COX enzymes. (**Figure 3)** shows the visualization of HOMO and LUMO of selected NSAIDs representing the location of frontier molecular orbitals in selected molecules.

For numerous DFT-calculated potential inhibitors, we have linked a few quantum chemical properties to how well they control inflammation. However, rather than reflecting the polarity of a single bond, the total dipole moment only captures the overall polarity of a molecule **(Table 4)**. It has been shown that as the inhibitors' dipole moments decrease, the effectiveness of the inhibition increases [27].

Table 4. The selected NSAIDs' estimated quantum chemical properties (HOMO, LUMO, HOMO-LUMO gap and dipole moment).

NSAIDs	HOMO (eV)	LUMO (eV)	HOMO-LUMO gap	Dipole moment (debye)
Aceclofenac	-0.2084	-0.0270	0.1814	1.9725
Antipyrine	-0.2047	-0.0246	0.1801	5.0950
Asprine	-0.2587	-0.0566	0.2021	2.3440
Celecoxib	-0.1594	-0.0329	0.1265	6.0950
Fenoprofen	-0.2176	-0.0070	0.2106	2.2060
Indomethacin	-0.2054	-0.0682	0.1372	2.3042

Table 5. Ionization potential, electron affinity, global hardness, softness, chemical potential, electrophilicity index of selected NSAIDs.

NSAIDs	Ionization potential	Electron affinity	Global hardness η	Softness σ	Electronegativity χ	Chemical potential μ	Electrophilicity index ω
Aceclofenac	0.2084	0.0270	0.0164	60.97	0.1177	-0.1177	0.2103
Antipyrine	0.2047	0.0246	0.0162	61.72	0.1146	-0.1146	0.2021
Asprine	0.2587	0.0566	0.0204	49.01	0.1576	-0.1576	1.333
Celecoxib	0.1594	0.0329	0.0080	125	0.0961	-0.0961	0.2875
Fenoprofen	0.2176	0.0070	0.0022	454	0.1053	-0.1053	1.25
Indomethacin	0.2054	0.0682	0.0094	106	0.1368	-0.1368	0.4973

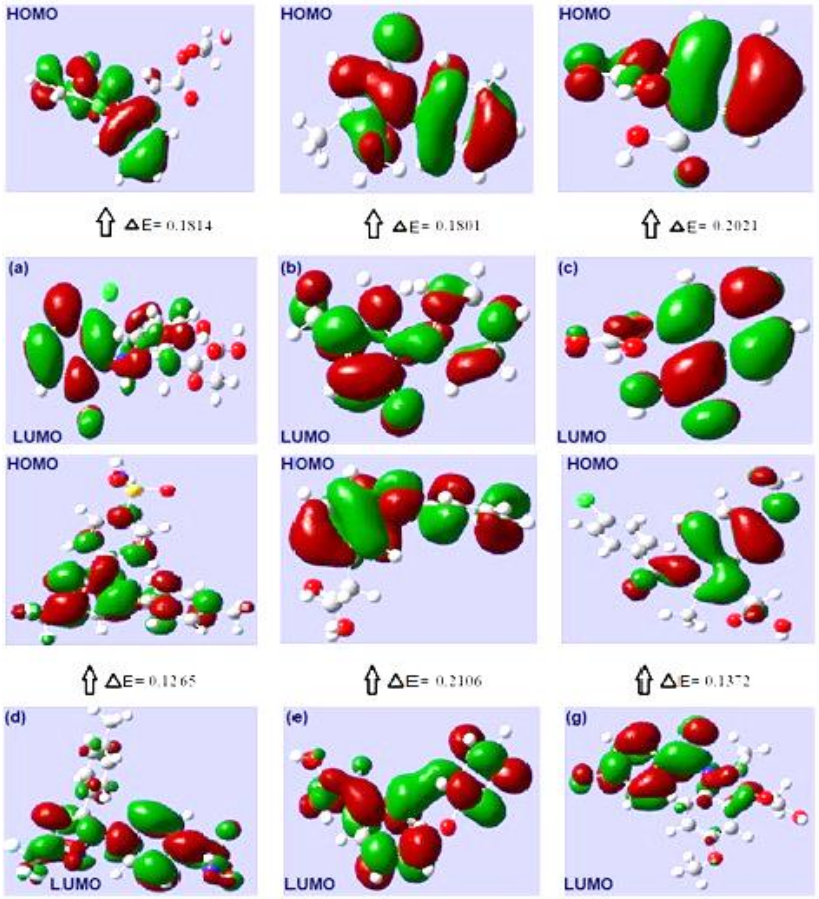

Fig. 3. HOMO and LUMO visualization of selected NSAIDs; (a) aceclofenac (b) antipyrine (c) aspirin (d) celecoxib (e) fenoprofen (g) indomethacin. Red and green colors are used to indicate the molecular orbital positive and negative phases, respectively.

The HOMO-LUMO energies, hardness, softness, and chemical potential of all compounds are presented in (**Table 5)**. The electronic absorption relates to the transition from the ground state to the first excited state and is mainly described by one electron excitation from HOMO to LUMO. The chemical hardness, softness, and potential values depend on the energy gap of HOMO-LUMO [28]. It is a useful analysis to study the reactivity of selected NSAIDs that an approaching electrophile will be attracted to negative regions (where the electron distribution effect is dominant). In MEP mapping, the maximum negative region which is the preferred site for electrophilic attack indicated by red color whereas, the maximum positive region which is the preferred site for nucleophilic attack is denoted by blue color. The importance of MEP lies in the fact that it simultaneously displays molecular size, and shape as well as positive, negative, and neutral electrostatic potential regions in terms of color grading **(Figure 4)**, and is very useful in research of molecular structure with its physiochemical property relationship. The different values of the electrostatic potential are represented by different colors and are graded as red < orange < yellow < green < blue [29].

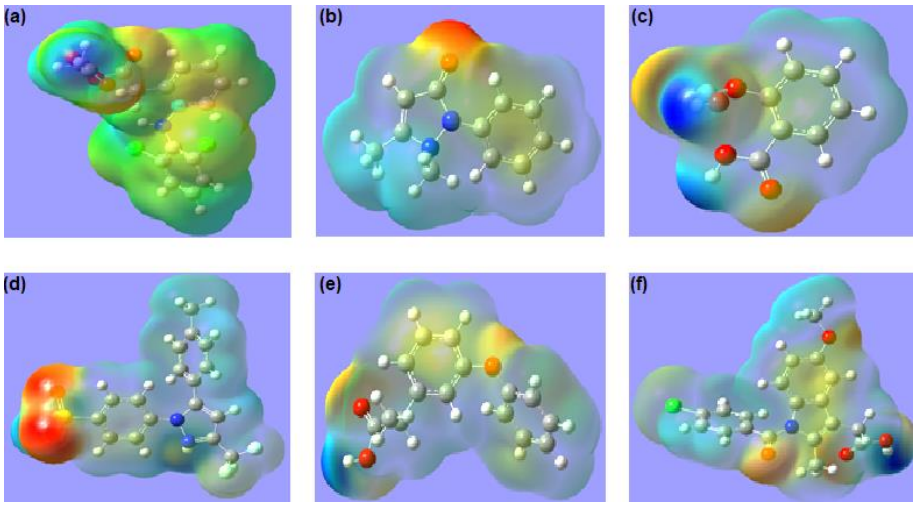

Fig. 4. MEP visualization of selected NSAIDs; (a) aceclofenac (b) antipyrine (c) aspirin (d) celecoxib (e) fenoprofen (f) indomethacin.

Discussion

The objective of the present study is to establish a correlation between computational and experimental outcomes for NSAIDs. The binding affinity of a ligand to its target enzyme is influenced by multiple factors, including electronic properties, molecular interactions, and structural stability. The binding energies of the ligands docked against COX-1 indicate that Fenoprofen (-7.4 kcal mol^{-1}) and Indomethacin (-7.4 kcal mol^{-1}) exhibit stronger binding affinities compared to Aspirin (-6.2 kcal mol^{-1}) and Antipyrine (-6.4 kcal mol^{-1}). A higher number of molecular interactions further supports the enhanced stability of Fenoprofen (8 interactions) and Indomethacin (11 interactions) within the active site of COX-1, whereas Aspirin and Antipyrine engage in fewer interactions (4 and 5, respectively), potentially leading to weaker binding. The experimental IC_{50} values provide further insight, with Indomethacin exhibiting the lowest IC_{50} (0.063 μM), suggesting potent COX-1 inhibition, while Fenoprofen has an intermediate IC_{50} of 36 μM. In contrast, Aspirin (1.3 μM) shows moderate inhibition, whereas Antipyrine has an IC_{50} value exceeding 1000 μM, indicating weak inhibition despite its relatively favorable binding energy. This discrepancy suggests that while computational binding energy provides a useful estimate of affinity, the actual inhibitory potency also depends on additional factors such as solubility, bioavailability, and ligand-induced conformational changes. Electronic properties play a crucial role in dictating ligand reactivity and interaction with the enzyme. The HOMO-LUMO gap, which represents the molecular reactivity, follows the trend Indomethacin (0.1372 eV) < Antipyrine (0.1814 eV) < Aspirin (0.1801 eV) < Fenoprofen (0.2106 eV). The smaller HOMO-LUMO gap of Indomethacin implies higher chemical reactivity, which aligns well with its high inhibitory potency (IC_{50} = 0.063 μM) and strong binding interactions. Fenoprofen, despite having strong binding energy, exhibits a higher HOMO-LUMO gap (0.2106 eV), suggesting lower electronic reactivity, which may contribute to its moderate inhibition. Similarly, Antipyrine, which has a moderate HOMO energy (-0.2047 eV) but a relatively large HOMO-LUMO gap, exhibits extremely weak inhibition, further highlighting the importance of electronic parameters in molecular docking predictions. The dipole moment provides insight into the polarity of the molecules, which affects their solubility and interaction within the active site. Antipyrine exhibits the highest dipole moment (5.0950 Debye), which may contribute to its weak binding by reducing its ability to establish hydrophobic interactions within COX-1. Aspirin (2.3440 Debye), Fenoprofen (2.2060 Debye), and Indomethacin (2.3042 Debye) have comparable dipole moments, but the significant difference in their inhibitory potency suggests that dipole moment alone is not the sole determinant of binding efficiency. The electrophilicity index (ω) is a measure of a molecule's ability to accept electrons and engage in interactions with biological targets. Aspirin has the highest electrophilicity index (1.333), which suggests strong electron-withdrawing potential, aiding in its interactions with COX-1. However, despite this high value, its binding energy is relatively weaker than Fenoprofen and Indomethacin, highlighting that while electrophilicity influences molecular interactions, other steric and structural factors also play significant roles in defining binding strength and inhibition. For COX-2 docking, a similar trend is observed. Fenoprofen (-7.6 kcal mol^{-1}) and Aceclofenac (-7.5 kcal mol^{-1}) exhibit the strongest binding affinities, whereas Celecoxib (-6.2 kcal mol^{-1}) and Aspirin (-6.1 kcal mol^{-1}) show weaker binding energies. However, experimental IC_{50} values indicate that Celecoxib (0.045 μM) is the most potent COX-2 inhibitor, followed by Aceclofenac (0.8 μM), Fenoprofen (1 μM), and Aspirin (5.9 μM). This observation reinforces the idea that while binding energy estimates the affinity of the ligand-enzyme complex, actual inhibitory potency is a function of multiple physicochemical factors, including solubility, bioavailability, and metabolic stability. Celecoxib exhibits the smallest HOMO-LUMO gap (0.1265 eV), suggesting higher electronic reactivity, which may contribute to its strong inhibition of COX-2 despite its moderate binding energy. In contrast, Fenoprofen has the largest HOMO-LUMO gap (0.2106 eV), indicating lower reactivity, which aligns with its relatively lower inhibitory potency (IC_{50} = 1 μM). The trend in electrophilicity index also supports these observations, with Celecoxib having a lower electrophilicity index (0.2875) than Aspirin (1.333) and Fenoprofen (1.25), indicating a different electronic interaction pattern that may enhance its specificity toward COX-2. The dipole moment significantly influences the binding of COX-2 inhibitors. Celecoxib has the highest dipole moment (6.0950 Debye), which may facilitate stronger polar interactions within the COX-2 active site, explaining its potent inhibition. Aceclofenac (1.9725 Debye) and Fenoprofen (2.2060 Debye) have lower dipole moments, which could limit their ability to form polar interactions, potentially affecting their overall potency. Aspirin, despite having a dipole moment of 2.3440 Debye, exhibits weak inhibition, further emphasizing that dipole moment alone does not dictate potency but works in conjunction with other molecular properties. Global hardness (η) and softness (σ) further provide insight into molecular stability and reactivity. Fenoprofen, with the lowest global hardness (0.0022 eV) and highest softness (454), is expected to be highly reactive, which supports its strong binding affinities to both COX-1 and COX-2. Celecoxib, which also exhibits low hardness (0.0080 eV) and high softness (125), follows a similar trend, explaining its high inhibitory potency. On the other hand, Aspirin, with higher global hardness (0.0204 eV) and lower softness (49.01), exhibits weaker binding and inhibition, reinforcing the role of electronic flexibility in ligand-enzyme interactions. Docking results indicate that all chosen NSAIDs exhibit physical interactions with the catalytic residues of both COX enzymes, thereby validating the experimental findings related to the inhibition of COX proteins by NSAIDs. MEP analysis further substantiates the interactions between NSAIDs and COX enzymes. In the MEP assay, regions with a maximum negative charge, denoted by a red color, were identified as the preferred sites for electrophilic attack, while regions with a maximum positive charge, marked by a blue color, were favored sites for nucleophilic attack. In summary, the computational and experimental data collectively highlight the intricate interplay between electronic properties, molecular interactions, and inhibitory potency. While strong binding energies generally correlate with lower IC_{50} values, exceptions occur due to factors such as the HOMO-LUMO gap, dipole moment, and electrophilicity, which influence molecular reactivity and interaction specificity. Celecoxib and Indomethacin emerge as the most potent inhibitors of COX-2 and COX-1, respectively, due to their optimal electronic properties and strong binding interactions. Fenoprofen, despite its strong binding energy, exhibits moderate inhibition, likely due to its larger HOMO-LUMO gap and lower electrophilicity. Aspirin, with weaker binding energies and higher global hardness, exhibits relatively lower potency against both enzymes. The analysis underscores the importance of integrating computational parameters with experimental validation to accurately predict ligand efficacy in drug design and enzyme inhibition studies.

4. Conclusions

Docking studies reveal that all selected NSAIDs generate stable protein-ligand complexes by developing non-covalent forces to the catalytic residues of COX proteins. DFT studies such as HOMO-LUMO, molecular electrostatic potential (MEP), and dipole moment validate the formation of stable protein-ligand complex systems. Regarding the inhibition of COX enzymes by chosen NSAIDs, computational results have been discovered to be congruent with experimental data retrieved from the literature. These results imply the validity of computational results and their potential use in computer-aided drug discovery.

Acknowledgments

The authors are grateful to the Department of Chemistry, Islamia College, Peshawar, KP, Pakistan for the provision of all facilities needed to execute the project. The authors are also thankful to Universidade Federal de Pelotas—UFPel, Pelota, RS, Brazil for providing support to perform this project.

Author Contributions

Ateeq Ullah Jan was responsible for conceptualization, data curation, and writing-review & editing; Khalid Khan for project administration, visualization, and formal analysis; Tanzeel Shah for validation and formal analysis; Nasir Ahmad for validation, data curation, and software; Haroon ur Rashid for writing-review & editing and software.

References and Notes

[1] Pinzi, L.; Rastelli, G. *Int. J. Mol. Sci.* **2019**, *20,* 4331. [Crossref]

[2] Grinter, S. Z.; Zou, X. *Molecules* **2014**, *19*, 10150. [Crossref]

[3] Mazurek, A. H.; Szeleszczuk, Ł.; Pisklak, D. M. *Pharmaceutics* **2020**, *12*, 415. [Crossref]

[4] Cramer, R. D.; Patterson, D. E.; Bunce, J. D. *J. Am. Chem. Soc.* **1988**, *110*, 5959. [Crossref]

[5] Grimme, S. *Wiley Interdiscip. Rev. Comput. Mol. Sci.* **2011**, *1*, 211. [Crossref]

[6] Gökce, H.; Bahçeli, S. *Spectrochim. Acta A Mol. Biomol. Spectrosc.* **2011**, *79*, 1783. [Crossref]

[7] Mitchell, J. A.; Akarasereenont, P.; Thiemermann, C.; Flower, R. J.; Vane, J. R. *Proc. Natl. Acad. Sci. U. S. A.* **1993**, *90*, 11693. [Crossref]

[8] Ricciotti, E.; FitzGerald, G. A.*; Arterioscler. Thromb. Vasc. Biol.* **2011**, *31*, 986. [Crossref]

[9] Boggara, M. B.; Krishnamoorti, R. *Biophys. J.* **2010**, *98*, 586. [Crossref]

[10] Jahnavi, K.; Reddy, P. P.; Vasudha, B.; Narender, B. *J. Drug Deliv. Ther.* **2019**, *9*, 442. [Crossref]

[11] Ur Rashid, H.; Xu, Y.; Ahmad, N.; Muhammad, Y.; Wang, L. *Bioorg. Chem*. **2019**, *87*, 335. [Crossref]

[12] Miciaccia, M.; Belviso, B. D.; Iaselli, M.; Cingolani, G.; Ferorelli, S.; Cappellari, M.; Loguercio P. P.; Perrone M. G.; Caliandro R.; Scilimati, A. *Sci. Rep.* **2021**, *11*, 4312. [Crossref]

[13] Rowlinson, S. W.; Kiefer, J. R.; Prusakiewicz, J. J.; Pawlitz, J. L.; Kozak, K. R.; Kalgutkar, A. S.; Stallings W. C.; Kurumbail R. G.; Marnett, L. J.; *J. Biol. Chem*. **2003**, *278*, 45763. [Crossref]

[14] RCSB Protein Data bank, **https://www.rcsb.org,** accessed in May **2024**.

[15] Labute, P.; Molecular Operating Environment (MOE), 2011. 10; Chemical Computing Group Inc., Montreal, QC, Canada, 2012.

[16] Evans, D. A.; Evans, S.; Rubenstein, S.; ChemDraw software v20.0; PerkinElmer Inc., Waltham, MA, USA; Evans, D. A. *Angew. Chem. Int. Ed*. **2014**, *53*, 11140. [Crossref]

[17] Brogden, R. N.; Wiseman, L. R. *Drugs* **1996**, *52*, 113. [Crossref]

[18] Ahnavi, K.; Reddy, P. P.; Vasudha, B.; Narender, B. *J. Drug Deliv. Ther.* **2019**, *9*, 442. [Crossref]

[19] Bombardier, C.; Laine, L.; Reicin, A.; Shapiro, D.; Burgos-Vargas, R.; Davis, B.; Day, R.; Ferraz, M. B.; Hawkey, C. J.; Hochberg, M. C.; Kvien, T. K.; Schnitzer, T. J. *N. Engl. J. Med.* **2000**, *343*, 1520. [Crossref]

[20] Gong, L.; Thorn, C. F.; Bertagnolli, M. M.; Grosser, T.; Altman, R. B.; Klein, T. E. *Pharmacogenet. Genomics* **2012**, *22*, 310. [Crossref]

[21] Brogden, R. N.; Pinder, R. M.; Speight, T. M.; Avery, G. S. *Drugs* **1977**, *13*, 241. [Crossref]

[22] Lucas, S. *Headache* **2016**, *56*, 436. [Crossref]

[23] Scholz, C.; Knorr, S.; Hamacher, K.; Schmidt, B. *J. Chem. Inf. Model*. **2015**, *55*, 398. [Crossref]

[24] Dennington, R.; Keith, T. A.; Millam, J. M.; GaussView, version 5; Semichem Inc., Shawnee Mission, KS, USA, 2016.

[25] Becke, A. D. *J. Chem. Phys.* **1993**, *98*, 5648. [Crossref]

[26] Koch, W.; Holthausen, M. C. In *A Chemist's Guide to Density Functional Theory*. 2nd ed. John Wiley & Sons: Berlin, Germany, 2001.

[27] Böhm, S.; Exner, O. *Phys. Chem*. **2004**, *6*, 510. [Crossref]

[28] Akman, F. *Cell. Chem Technol*. **2019**, *53*, 243. [Crossref]

[29] Suresh, C. H.; Remya, G. S.; Anjalikrishna, P. K. *Wiley Interdiscip. Rev. Comput. Mol. Sci.* **2022**, *12*, e1601. [Crossref]

How to cite this article

Jan, A. U.; Khan, K.; Shah, T.; Ahmad, N.; Rashid, H. U. *Orbital: Electronic J. Chem*. **2025**, *17*, 7. DOI: **http://dx.doi.org/10.17807/orbital.v17i1.21586**